Asian Journal of Chemistry; Vol. 36, No. 11 (2024), 2622-2628

ASIAN JOURNAL OF CHEMISTRY

https://doi.org/10.14233/ajchem.2024.32609

One Pot Green Synthesis of Zr doped NiO Nanoparticles using *Annona squamosa* Seed Extract: Characterization and Biological Properties

M. KARTHIKEYAN*, M. PRIYADHARSHAN, R. KEERTHANA, T. VASIKARAN and A. MANOHAR

Department of Chemistry, Periyar Maniammai Institute of Science and Technology (Deemed to be University), Vallam, Thanjavur-613403, India

*Corresponding author: E-mail: karthichemist10@gmail.com

Received: 30 August 2024; *Accepted*: 18 October 2024; *Published online*: 30 October 2024; AJC-21799

Pure and Zr-doped NiO nanoparticles were successfully synthesized through green synthesis using extract of *Annona squamosa* seeds. The synthesized nanoparticles were characterized by X-ray diffraction (XRD), Fourier transform infrared (FTIR) spectroscopy, UV-vis spectroscopy, field emission scanning electron microscopy (FESEM), EDAX (energy dispersive X-ray analysis) and elemental mapping analysis. The addition of zirconium dopant has been integrated into the single-phase NiO lattice structure as indicated by characterization findings. Furthermore, the antibacterial, antifungal and antioxidant properties of Zr-doped and undoped NiO NPs were thoroughly examined. As a result of the strong Zr-doped NiO NPs synergistic effect, the results showed that the Zr-doped NiO NPs have improved the biomedical properties when compared to the undoped NiO NPs. The optimized size and shape of the nanoparticles contributed significantly to their improved effectiveness against the microorganisms and oxidative stress.

Keywords: Zr-NiO nanoparticles, Green synthesis, Antimicrobial activity, Antioxidant property, Antifungal activity.

INTRODUCTION

Metal oxide nanoparticles have emerged as a focal point of research in recent years, owing to their unique blend of properties that make them incredibly versatile. With their expansive surface area, stable band gap and potential for reuse, these nanoparticles have proven to be highly attractive for a multitude of applications, showcasing their remarkable utility [1]. Nickel oxide nanoparticles (NiO NPs) have garnered significant interest in recent years due to their exceptional versatility, stemming from their unique combination of properties. These properties, including their optical, electrical and magnetic characteristics, make NiO NPs highly adaptable and suitable for a wide range of applications such as energy storage, biomedical assays and environmental remediations [2-4]. Zirconium-doped nickel oxide (Zr-doped NiO) nanoparticles exhibit enhanced optical, electrical, magnetic and catalytic properties, making them suitable for various applications including energy storage, environmental remediation and biomedicines [5]. Zr-doped NiO NPs were found to be significantly enhanced, with a specific capacitance of 735.46 F g^{-1}, indicating their potential suitability for energy storage applications [6]. The synthesis of NiO NPs has been achieved through a range of techniques, each with its own strengths and applications. These methods include sol-gel processing, solvothermal synthesis, hydrothermal treatment, thermal decomposition and precipitation, enabling researchers to fine the characteristics of NiO NPs for various applications [1,7]. Among these, green synthesis of nanoparticles offers several merits, including reduced toxicity, environmental sustainability, cost-effectiveness and scalability, making it a promising approach for large-scale production of nanoparticles [8-10].

Biocompatible metal oxide nanoparticles are synthesized through a reduction process mediated by metabolites, which enables the transformation of metal ions into their corresponding nanostructured metal oxides [1]. *Annona squamosa* L., commonly known as sugar apple, was chosen for this study due to its therapeutic values and belongs to *Annonaceae* family. The *Annonaceae* family, also referred to as the custard apple family, is recognized for its diverse medicinal properties, including antiulcer, anticonvulsant and antibacterial activities, which have been extensively studied. Furthermore, a wide range of pharmacological properties, such as analgesic, antimicrobial, anti-inflammatory, cytotoxic, antioxidant, anti-lipidemic, antitumor, hepatoprotective, larvicidal, insecticidal and anthelmintic

activities, have been exhibited by *A. squamosa* L. [11,12]. The biological activities of metal oxide nanoparticles, including antibacterial properties, have been enhanced through the doping of various metals. Moreover, the potential of metal-doped nanoparticles to modulate ROS formation has been harnessed for anticancer applications, resulting in the induction of cytotoxicity in cancer cells [13,14].

The present study reports a biocompatibility assisted synthesis of pure NiO NPs and Zr doped NiO NPs facilitated by the use of aqueous seed extract of *A. squamosa* L. The phytochemicals presented in seed serving as capping and stabilizing agents (D-glucose, ascorbic acid and quercetin) and also enhance the biological activity of nanoparticles. The biosynthesized Zr-doped NiO NPs was confirmed through various characterization techniques, including XRD, UV-DRS, FT-IR, FESEM-EDX and mapping analysis. Furthermore, the biological activities of the biosynthesized nanoparticles from *A. squamosa* L. were investigated through antibacterial, antifungal studies as well as antioxidant capacity.

EXPERIMENTAL

Synthesis of *A. squamosa* L. mediated nano-particles: A two-step synthesis process utilizing *A. squamosa* L. seed extract was employed to produce NiO NPs and Zr-doped NiO NPs. The process commenced with boiling the seed powder in water to prepare the extract, which was then combined with 0.1 M $NiCl_2$ solution and stirred to yield a precipitate. The precipitate was subsequently dried and annealed to obtain pure NiO NPs. To synthesize Zr-doped NiO NPs, 0.003 M zirconium oxychloride was added to 0.097 M $NiCl_2$ solution, along with the seed extract, which served as a reducing and stabilizing agent. The process was repeated to obtain the Zr-doped NiO NPs.

Characterization: The NiO and Zr doped NiO NPs were characterized by powder X-ray diffractometer (model: X'PERT PRO PAN analytical). The diffraction pattern was recorded in the range of 25-80º, at the monochromatic wavelength of 1.54 Å. The morphology of the synthesized nanoparticles was examined using FESEM. Gemini 300 (Carl Zeiss) instrument was used to examine the samples' surface properties. The NiO NPs were analyzed by EDAX (model: ULTRA 55). The FT-IR spectrum was recorded in the range of 4000-400 cm^{-1} by using Perkin-Elmer spectrometer and the ultraviolet-visible spectra of NiO NPs were recorded on a Perkin-Elmer UV-Lambda 25 spectrophotometer (Perkin-Elmer, USA).

Antimicrobial activity: The antibacterial activity of the prepared NiO and Zr doped NiO nanomaterials were employed by using the agar well-diffusion method and tested against Gram-positive (*S. aureus*) and Gram-negative (*E. coli*) bacterial strain [15]. A 100 mL of fresh culture containing 1×10^8 CFU/mL of bacteria was spread onto the Mueller Hinton Agar (MHA) plates using the sterile swab. The perti-plate was tested at 60 µL of NiO and Zr doped NiO nanomaterial dispersed separately in DMSO solvent. Zone of inhibition levels (mm) was measured subsequently for 24 h at 37 ºC. For positive control, standard antibiotic streptomycin (10 µg disc) was used [15].

Antifungal activity: Antifungal activity was determined using potato dextrose agar by using a well diffusion method against the test fungi *C. albicans* and *Aspergillus niger* [16]. The test strain was transferred into potato dextrose broth (PDB) and incubated at 30 ºC. Subsequently, a well-loaded with 60 µL of test samples (pure NiO and Zr doped NiO NPs) was placed onto the inoculated plates using sterile forceps and incubated at 30 ºC for 24 h under visible light. Zone of inhibition levels (mm) was measured subsequently for 24 h at 37 ºC. For positive control, standard antibiotic fluconazole (10 µg disc) was used.

Antioxidant activity: The effect of pure and Zr doped NiO NPs on DPPH radical was estimated using reported method [17]. About 0.1 mL of DPPH methanol solution (0.135 mM) was mixed with 1.0 mL of different concentrations of pure NiO and Zr doped NiO NPs samples. The reaction mixture was vortexed thoroughly and left in the dark at room temperature for 30 min. The absorbance of the mixture was measured spectrophotometrically at 517 nm. Vitamin C was used as standard drug [17]. The percentage of free radical scavenging was calculated according to the following equation:

$$\text{Scavenging (\%)} = 100 - \left(\frac{A_{sample} - A_{blank}}{A_{control}} \right) \times 100$$

RESULTS AND DISCUSSION

PXRD studies: Fig. 1 illustrates the powder XRD spectra of pure NiO and Zr doped NiO NPs. The XRD spectra reveals that all the samples exhibit a face-centered cubic (FCC) crystal structure, indicating a uniform crystallization pattern across the samples. The X-ray diffraction peaks in the obtained spectra are perfectly matched to the crystal planes (111), (200), (220), (311) and (222), aligning with the standard JCPDS card No. 73-1523. The XRD patterns are characterized by a single-phase structure, with all peaks perfectly indexed, confirming the high purity of the sample and the absence of any secondary phases or unwanted impurities, indicating that doping has not caused any structural modifications [6]. A shift of the high intensity

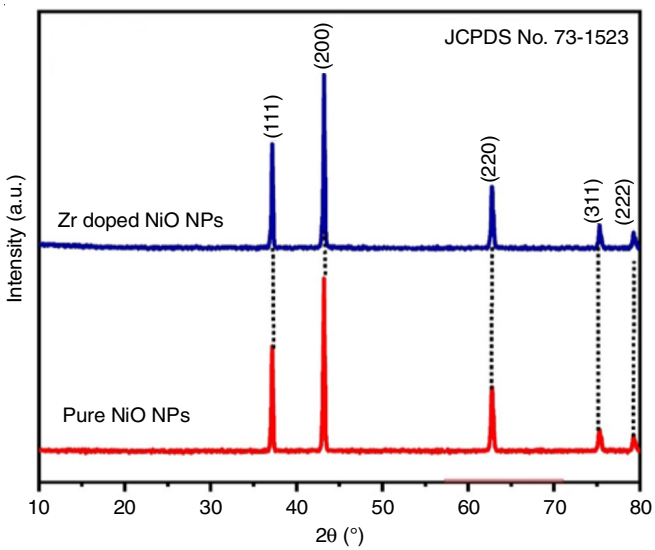

Fig. 1. PXRD pattern of pure NiO and Zr doped NiO NPs

peak of Zr doped NiO NPs is revealed by the XRD pattern, compared to pure NiO, confirming a change in the lattice constants [18]. The average crystallite size of pure NiO and Zr doped NiO NPs was calculated to be 45 nm and 40 nm, using the Scherrer's formula:

$$D = \frac{0.9\lambda}{\beta\cos\theta} \quad (1)$$

The broadening of the full width at half maximum (FWHM) is attributed to the substitution of smaller Ni^{2+} ions (0.72 Å) with larger Zr^{4+} ions (0.79 Å). Additionally, the XRD pattern of Zr-doped NiO NPs exhibits a slight shift of diffraction peaks towards lower angles, indicating the incorporation of Zr into the NiO lattice, compared to pure NiO NPs [6,19].

FT-IR spectral studies: Fig. 2 illustrates the FT-IR spectrum of the as-synthesized NPs, encompassing a broad wavenumber range of 4000-400 cm^{-1}, which provides a detailed fingerprint of the molecular structure and functional groups present in the nanoparticles. The FT-IR spectra of pure NiO and Zr doped NiO NPs exhibit the characteristic absorption bands at 3444, 1649, 579 and 487cm^{-1}, indicating the presence of distinct functional groups. The absorption bands at 3444 cm^{-1} and 1649 cm^{-1} are attributed to the stretching and bending vibrations of the O-H bond, respectively. The FT-IR absorption peak at 491 cm^{-1} is attributed to the stretching vibration of the Ni-O bond and exhibits broadening after Zr doping in the NiO lattice, shifted to 484 cm^{-1}, which suggests a modification in the lattice structure and bonding environment around the Ni ions due to Zr incorporation [6,20].

Absorbance and bandgap studies: The UV-Vis absorption spectra of pure NiO and Zr doped NiO NPs are depicted in Fig. 3a-b in the spectral range of 200-800 nm. The pure NiO NPs exhibits an absorption peak at 388 nm, which shifts

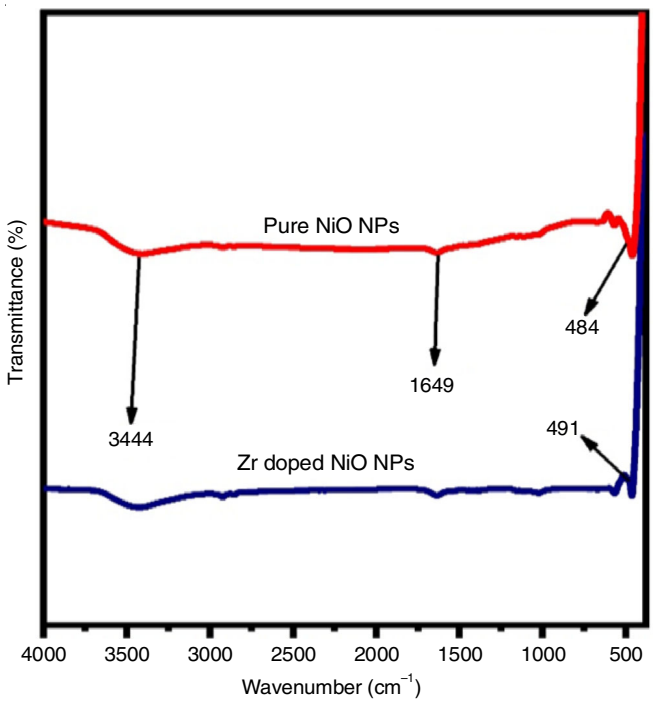

Fig. 2. FT-IR spectra of pure NiO and Zr doped NiO NPs

to a higher wavelength of 395 nm for Zr doped NiO NPs with the addition of Zr, as shown in Fig. 3b. The doping of Zr into the NiO lattice results in enhanced absorbance, significantly influencing the materials band gap, surface morphology and defect concentration, with important implications for its optical and electronic properties [6,21]. Alternatively, the optical bandgap energy can be determined using Tauc's plot relations, which correlate the incident photon energy (hν) with the absorption coefficient (α) through the following relationship:

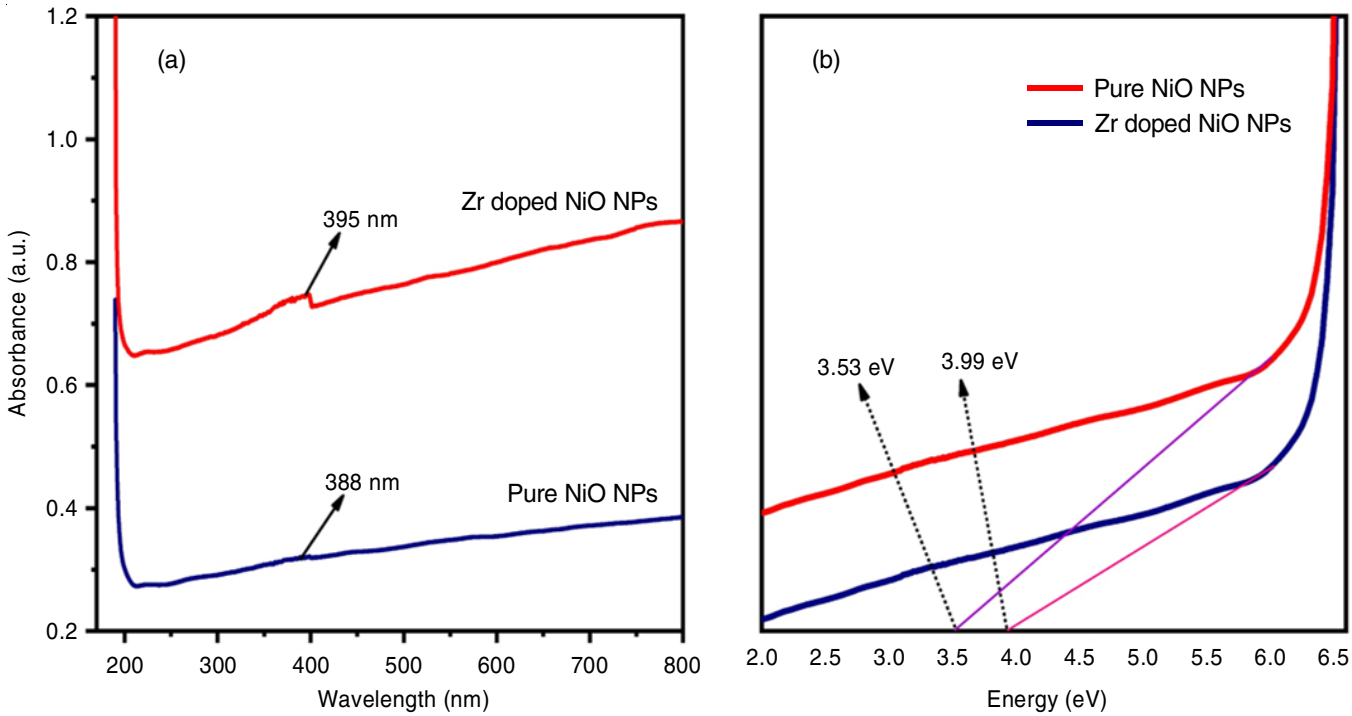

Fig. 3. UV absorbance and band gap spectra of pure NiO and Zr doped NiO NPs

$$\alpha h\nu = A\,(h\nu - E_g)^n \quad (2)$$

where α is the absorption coefficient, hν is the photon energy, A is a constant, E_g is the optical bandgap energy and n is a power factor that depends on the transition type. The bandgap energies were obtained by linearly extrapolating the $(\alpha h\nu)^2$ *versus* hν plots to zero, resulting in E_g values of 3.53 eV for pure NiO and 3.99 eV for Zr doped NiO NPs. The observed decrease in bandgap energy upon zirconium doping suggests a modification of the materials electronic structure, leading to enhanced optical absorption in the Zr-doped NiO NPs [22].

FESEM-EDAX and mapping studies: Fig. 4a-b display the surface morphology of pure NiO and Zr doped NiO NPs. The FE-SEM micrograph reveals uniform distribution of nanoparticles with small agglomeration in pure NiO nanoparticles. Following this, agglomeration reduces with the Zr-doping and the grains attain rhombus shape. This observation suggests that Zr-doping has a profound impact on the surface morphology, significantly influencing the nucleation process and resulting in a more substantial change in the surface structure. Furthermore, the elemental mapping analysis (Fig. 4c-f) confirms the presence of the expected elements, namely Ni, Zr and O, in the composition of the nanoparticles, as anticipated [23,24].

The EDAX spectra for pure NiO and Zr doped NiO NPs (Fig. 5) reveal the presence of nickel (Ni), zirconium (Zr) and oxygen (O) atoms in a well-defined and expected stoichiometric ratio, confirming their successful incorporation into the NPs [6,25].

Biomedical applications

Antimicrobial studies: The disc diffusion method was employed to investigate the antibacterial properties of pure NiO

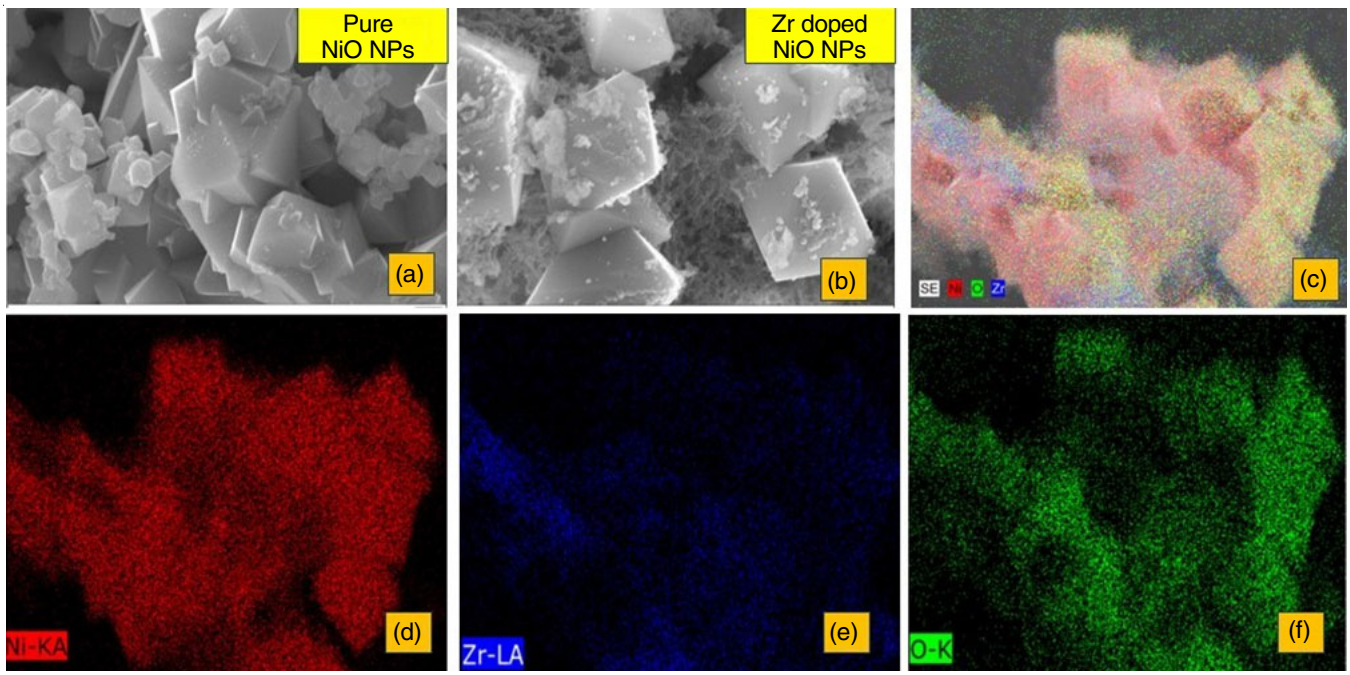

Fig. 4. FESEM and mapping spectra of pure NiO and Zr doped NiO NPs

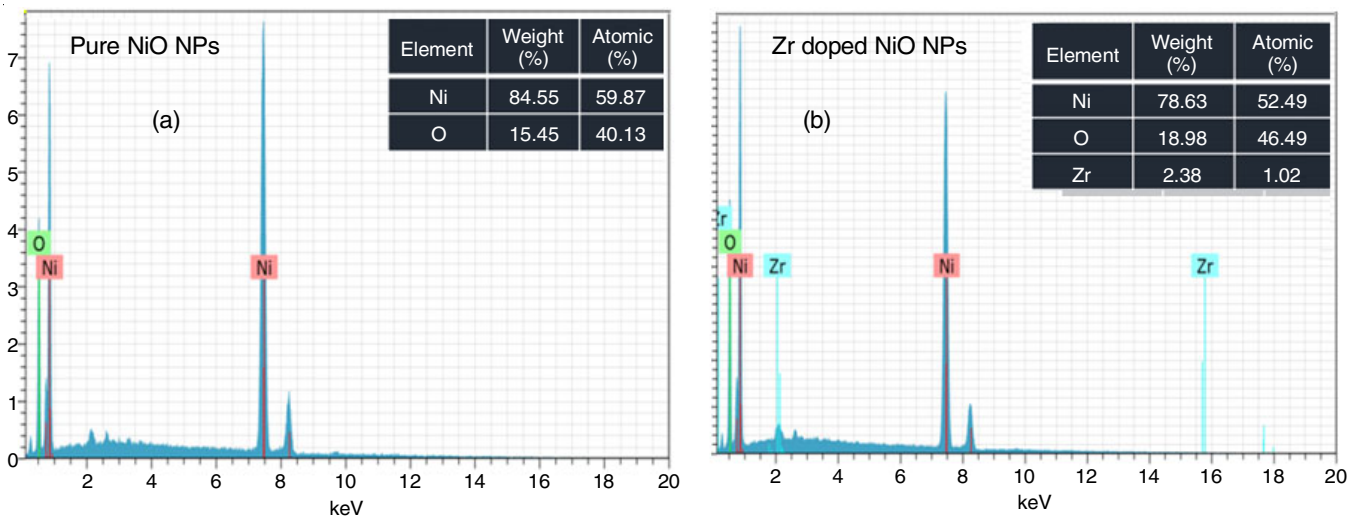

Fig. 5. EDAX spectra of pure NiO and Zr doped NiO NPs

and Zr doped NiO NPs against two clinically relevant pathogens, *Staphylococcus aureus* (Gram-positive) and *Escherichia coli* (Gram-negative) using streptomycin as the standard antibiotic. The antibacterial properties of the synthesized nanoparticles are evident in Fig. 6, which shows the inhibition of *S. aureus* and *E. coli* growth. From the assay, the zone of inhibition results from combined effects of cell membrane disruption, ROS production, Ni and Zr ion release. This synergy leads to loss of the cellular viability and inhibition of cell division. Ultimately, bacterial cells succumb to death [26-28]. The corresponding mean inhibition zone values demonstrate that Zr-doping enhances the antimicrobial activity of NiO nanoparticles against *S. aureus* and *E. coli*, with increased zones of inhibition.

Antifungal studies: The biocompatible synthesis of pure NiO and Zr doped NiO NPs nanoparticles yielded promising antifungal results. The zone of inhibition values indicated that these nanoparticles exhibit considerable antifungal activity against two prominent fungal pathogens, *Candida albicans* and *Aspergillus niger* (Fig. 7). The observed growth inhibition zones were comparable to those achieved with streptomycin, a well-established antifungal agent. Zr-doped NiO nanoparticles exhibit potent antifungal activity against *C. albicans* and *A. niger*. The Zr doping enhances surface properties, electrostatic interactions and cellular disruption, leading to improved efficacy. The fungicidal activity of NiO NPs is substantially augmented by Zr doping, resulting in enhanced inhibition of fungal growth and increased cellular toxicity [29-31]. Comparative studies reveal a significant increase in antifungal efficacy, underscoring the benefits of Zr incorporation. These findings suggest Zr-doped NiO NPs as a promising nanomaterial for antifungal therapies.

Antioxidant assay: The free radical scavenging potential of biosynthesized pure NiO and Zr doped NiO NPs, derived from *A. squamosa* seed extract, was evaluated using DPPH assay to assess their antioxidant efficacy. The antioxidant assay revealed a dose-dependent increase in radical scavenging capacity, with nanoparticles demonstrating potent antioxidant potential. A dose-response study was conducted to evaluate the scavenging activities of pure NiO and Zr doped NiO NPs at concentrations of 1-10 µg/mL, in increment of (1 µg, 2.5 µg, 5 µg, 7.5 µg and 10 µg) depicted in Table-1. From the analysis, Zr doped NiO NPs exhibited significant antioxidant activity, as evidenced by their ability to scavenge DPPH radicals (Fig. 8). The DPPH assay revealed a concentration-dependent increase in antioxidant activity, indicating potent radical scavenging potential.

The Zr doped NiO NPs exhibited significant antioxidant activity as evidenced by their ability to scavenge DPPH radicals.

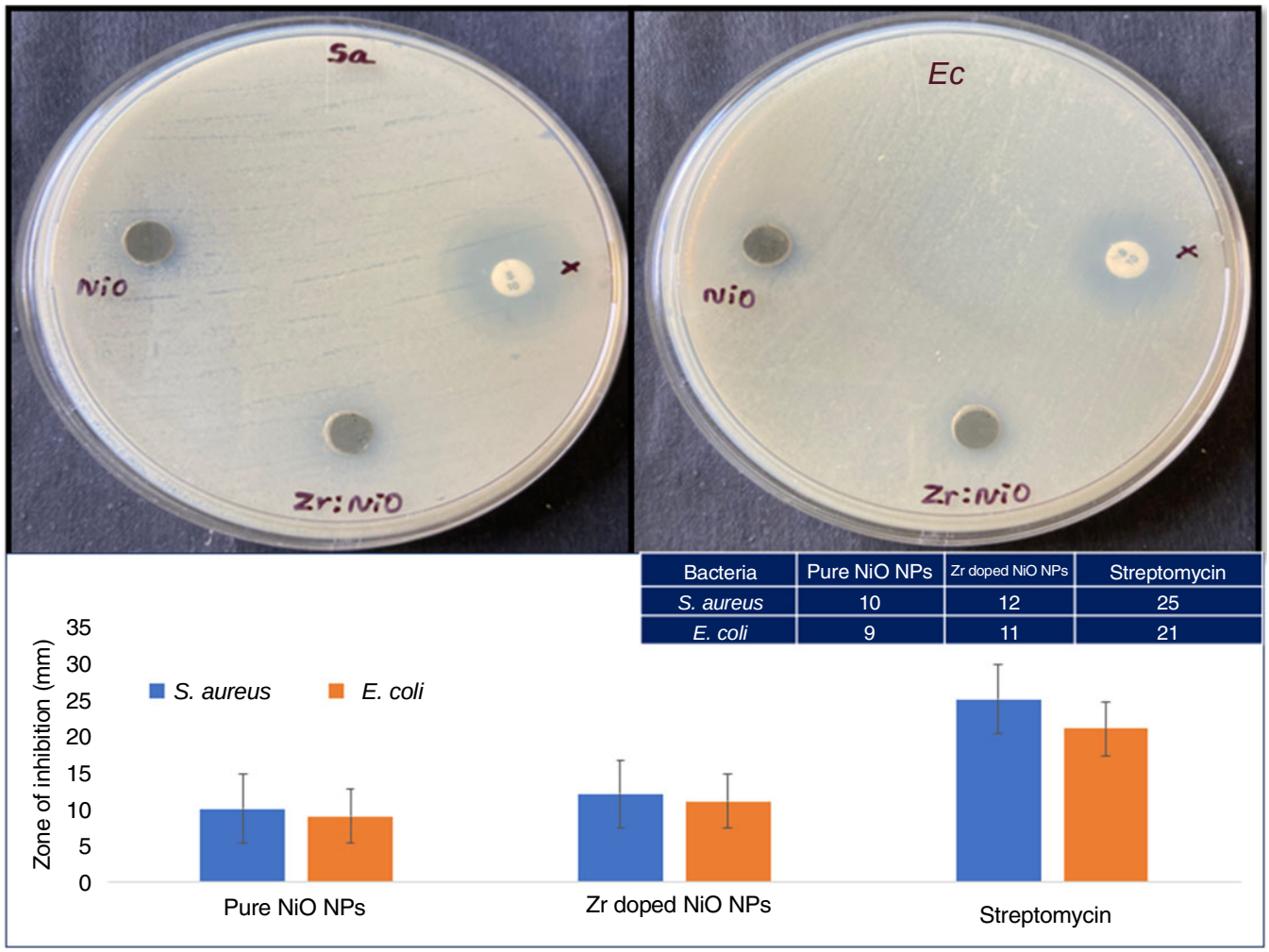

Fig. 6. Antibacterial effect of pure NiO and Zr doped NiO NPs against *S. aureus* and *E. coli*

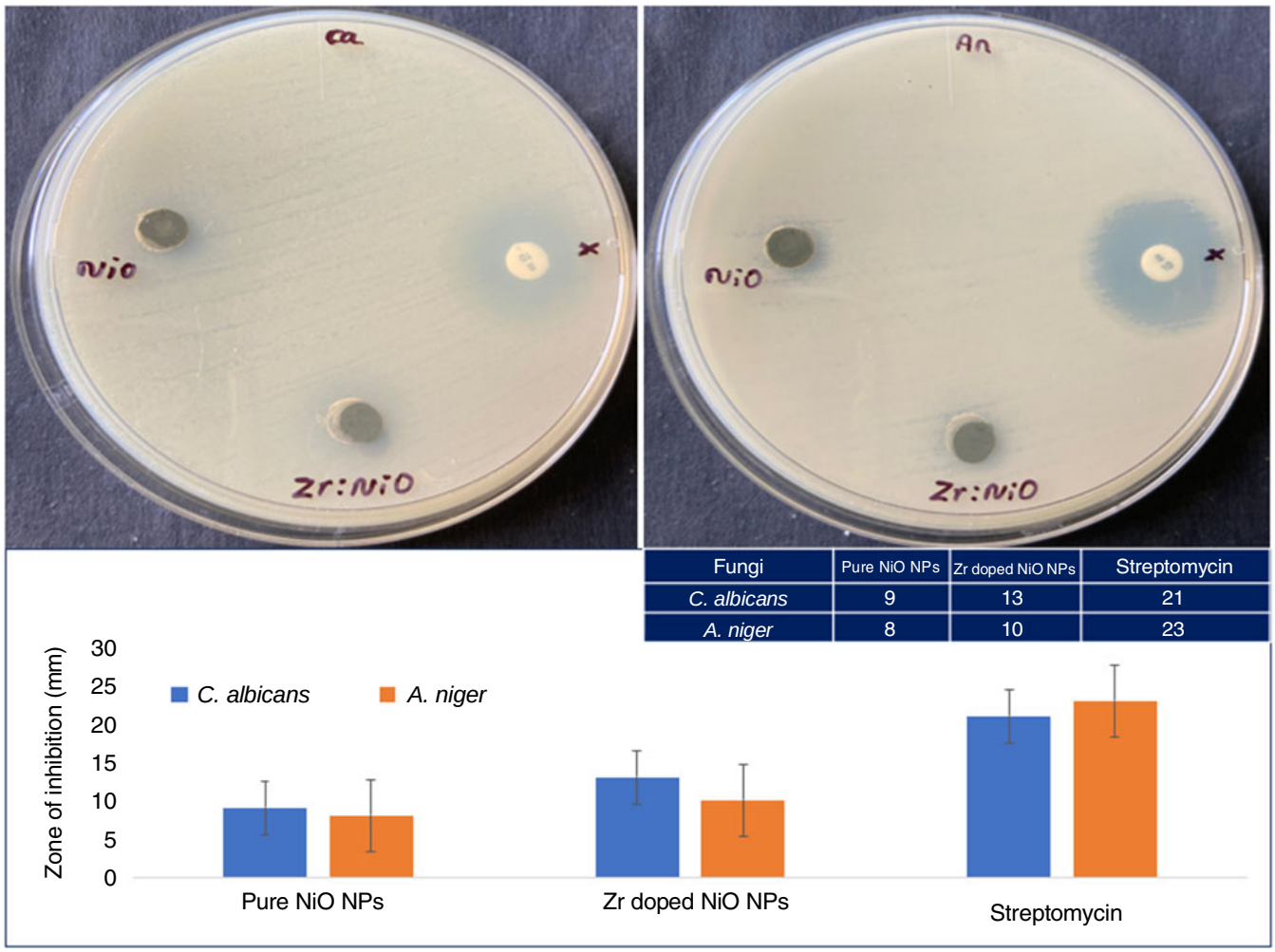

Fig. 7. Antifungal effect of pure NiO and Zr doped NiO NPs against *C. albicans* and *Aspergillus niger*

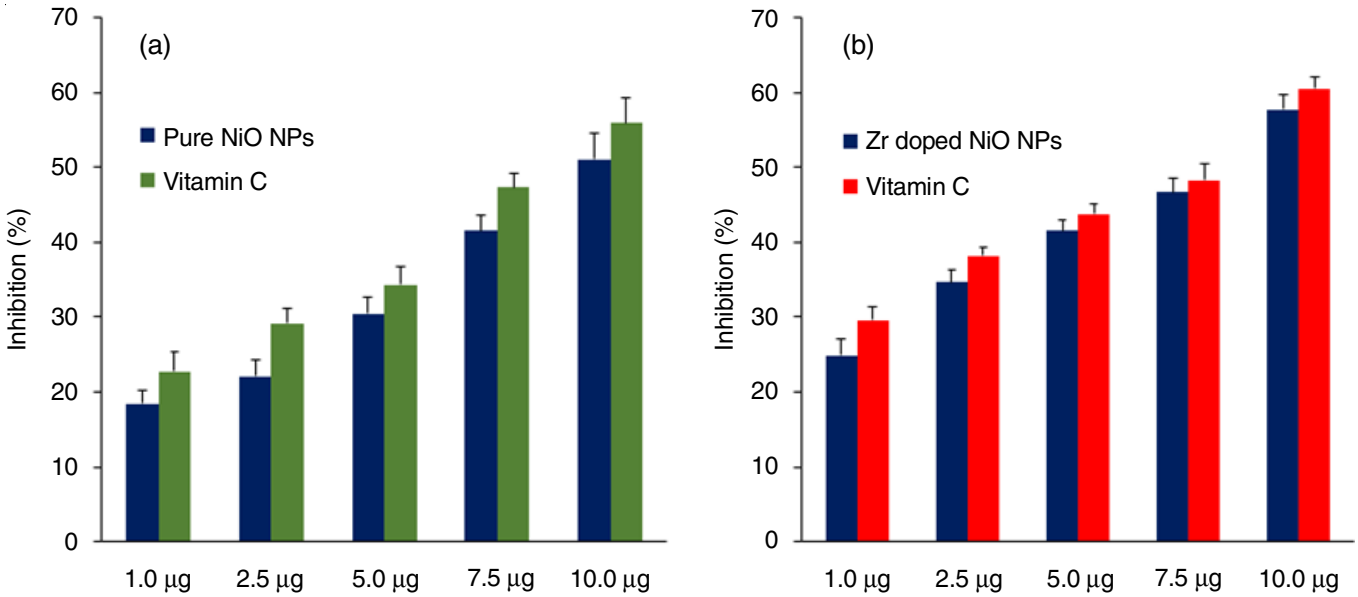

Fig. 8. Antioxidant assay 2,2-diphenyl-1-picrylhydrazyl (DPPH) radical of pure NiO and Zr doped NiO NPs

The DPPH assay revealed a concentration-dependent increase in antioxidant activity, indicating potent radical scavenging potential (Fig. 8). Significantly, the Zr doping enhanced the antioxidant activity of NiO NPs, suggesting a synergistic effect. Zirconium doping unlocks enhanced reactivity, making nanoparticles effective free radical quenchers [32-34]. These results

TABLE-1
COMPARATIVE ANTIOXIDANT CAPACITY OF PURE NiO NPs AND Zr DOPED NiO NPs AT DIFFERENT CONCENTRATIONS

Conc. (µg)	Pure NiO NPs	Vitamin-C (Ref)	Zr doped NiO NPs	Vitamin-C (Ref)
1.0	18.446	22.813	24.863	29.65
2.5	22.135	29.159	34.664	38.220
5.0	30.485	34.305	41.560	43.822
7.5	41.553	47.341	46.642	48.270
10.0	51.067	55.917	57.713	60.461

suggest that Zr-doped NiO could be a promising material for applications requiring antioxidant properties, such as biomedical devices, environmental remediation and cosmetic products.

Conclusion

In this research, we achieved the green synthesis of pure and Zr-doped NiO NPs using *Annona squamosa* L. seed extract as stabilizing agent. Several characterization techniques confirmed the successful incorporation of zirconium into the NiO crystal structure. Remarkably, Zr-doped NiO NPs displayed superior antibacterial and antifungal activity compared to their undoped counterparts, owing to the synergistic influence of Zr doping. The tailored size and shape of the nanoparticles, achieved through the synthesis process, played a crucial role in enhancing their efficacy against microbial, fungal growth and oxidative stress. These findings demonstrated the remarkable efficacy of Zr-doped NiO nanoparticles as antimicrobial, antifungal and antioxidant agents, paving the way for transformative advancements in biomedical and environmental technologies.

ACKNOWLEDGEMENTS

The financial assistance received in the form of seed money grant (Lr. No: 41/Registrar/2022-23/Date: 30.03.2023) from Periyar Maniammai Institute of Science and Technology (Deemed to be University), Thanjavur, India is greatly acknowledged.

CONFLICT OF INTEREST

The authors declare that there is no conflict of interests regarding the publication of this article.

REFERENCES

1. K. Lingaraju, H. Raja Naika, H. Nagabhushana, K. Jayanna, S. Devaraja and G. Nagaraju, *Arab. J. Chem.*, **13**, 4712 (2020); https://doi.org/10.1016/j.arabjc.2019.11.003
2. B.A. Abbasi, J. Iqbal, T. Mahmood, R. Ahmad, S. Kanwal and S. Afridi, *Mater. Res. Express*, **6**, 0850a7 (2019); https://doi.org/10.1088/2053-1591/ab23e1
3. I. Shaheen, K.S. Ahmad, C. Zequine, R.K. Gupta, A.G. Thomas and M.A. Malik, *Int. J. Energy Res.*, **44**, 5259 (2020); https://doi.org/10.1002/er.5270
4. T. Ali, M.F. Warsi, S. Zulfiqar, A. Sami, S. Ullah, A. Rasheed, I.A. Alsafari, P.O. Agboola, I. Shakir and M.M. Baig, *Ceram. Int.*, **48**, 8331 (2022); https://doi.org/10.1016/j.ceramint.2021.12.039
5. G. Rajesh, S. Akilandeswari, D. Govindarajan and K. Thirumalai, *Mater. Res. Express*, **6**, 1050a9 (2019); https://doi.org/10.1088/2053-1591/ab405e
6. M.M. Shah, D.K. Gupta, R.N. Ali, S. Husain and M.U.D. Rather, *Chem. Zvesti*, **78**, 2987 (2024); https://doi.org/10.1007/s11696-023-03287-0
7. M.I. Din and A. Rani, *Int. J. Anal. Chem.*, **2016**, 1 (2016); https://doi.org/10.1155/2016/3512145
8. A.A. Ezhilarasi, J.J. Vijaya, K. Kaviyarasu, M. Maaza, A. Ayeshamariam and L.J. Kennedy, *J. Photochem. Photobiol. B*, **164**, 352 (2016); https://doi.org/10.1016/j.jphotobiol.2016.10.003
9. S.S. Salem and A. Fouda, *Biol. Trace Elem. Res.*, **199**, 344 (2021); https://doi.org/10.1007/s12011-020-02138-3
10. C. Hano and B.H. Abbasi, *Biomolecules*, **12**, 31 (2021); https://doi.org/10.3390/biom12010031
11. J. Pathak, *Biosci. Biotechnol. Res. Commun.*, **14**, 397 (2021); https://doi.org/10.21786/bbrc/14.1/56
12. V. Jose, L. Raphel, K.S. Aiswariya and P. Mathew, *Bioprocess Biosyst. Eng.*, **44**, 1819 (2021); https://doi.org/10.1007/s00449-021-02562-2
13. R.U.K. Shenoy, A. Rama, I. Govindan and A. Naha, *OpenNano*, **8**, 100070 (2022); https://doi.org/10.1016/j.onano.2022.100070
14. S. Laurent, D. Forge, M. Port, A. Roch, C. Robic, L. Vander Elst and R.N. Muller, *Chem. Rev.*, **108**, 2064 (2008); https://doi.org/10.1021/cr068445e
15. J.J. Rojas, V.J. Ochoa, S.A. Ocampo and J.F. Muñoz, *BMC Complement. Altern. Med.*, **6**, 2 (2006); https://doi.org/10.1186/1472-6882-6-2
16. W. Huang, H. Fang, S. Zhang and H. Yu, *Micro & Nano Lett.*, **16**, 374 (2021); https://doi.org/10.1049/mna2.12060
17. C.M. Liyana-Pathirana and F. Shahidi, *J. Agric. Food Chem.*, **53**, 2433 (2005); https://doi.org/10.1021/jf049320i
18. M. Sun, Z. Li, H. Li, Z. Wu, W. Shen and Y.Q. Fu, *Electrochim. Acta*, **331**, 135366 (2020); https://doi.org/10.1016/j.electacta.2019.135366
19. W. Ahmed and J. Iqbal, *Ceram. Int.*, **47**, 24895 (2021); https://doi.org/10.1016/j.ceramint.2021.05.216
20. M. Abdur Rahman and R. Radhakrishnan, *SN Appl. Sci.*, **1**, (2019); https://doi.org/10.1007/s42452-019-0232-y
21. S. Saiganesh, T. Krishnan, G. Narasimha, H.S. Almoallim, S.A. Alhari, L.V. Reddy, K. Mallikarjuna, A. Mohammed and V.S.V. Prabhakar, *Crystals*, **11**, 124 (2021); https://doi.org/10.3390/cryst11020124
22. S.G. Firisa, G.G. Muleta and A.A. Yimer, *ACS Omega*, **7**, 44720 (2022); https://doi.org/10.1021/acsomega.2c04042
23. I. Khan, S. Khan, R. Nongjai, H. Ahmed and W. Khan, *Opt. Mater.*, **35**, 1189 (2013); https://doi.org/10.1016/j.optmat.2013.01.019
24. S. Agrawal, A. Parveen and A. Azam, *J. Lumin.*, **184**, 250 (2017); https://doi.org/10.1016/j.jlumin.2016.12.035
25. S. Suthakaran, S. Dhanapandian, N. Krishnakumar, N. Ponpandian, P. Dhamodharan and M. Anandan, *Mater. Sci. Semicond. Process.*, **111**, 104982 (2020); https://doi.org/10.1016/j.mssp.2020.104982
26. P. Muthukumaran, C.V. Raju, C. Sumathi, G. Ravi, D. Solairaj, J. Wilson, P. Rameshthangam, S. Rajendran and S. Alwarappan, *New J. Chem.*, **40**, 2741 (2016); https://doi.org/10.1039/C5NJ03539B
27. N.Y. Elamin, T. Indumathi and E.R. Kumar, *Physica E*, **142**, 115295 (2022); https://doi.org/10.1016/j.physe.2022.115295
28. M.W. Alam, A. BaQais, T.A. Mir, I. Nahvi, N. Zaidi and A. Yasin, *Sci. Rep.*, **13**, 1328 (2023); https://doi.org/10.1038/s41598-023-28356-y
29. M. Bhoye, S. Pansambal, P. Basnet, K.-Y.A. Lin, K.Y. Gutierrez-Mercado, A. Pérez-Larios, A. Chauhan, R. Oza and S. Ghotekar, *J. Compos. Sci.*, **7**, 105 (2023); https://doi.org/10.3390/jcs7030105
30. I. Kumar, B. Yaseen, C. Gangwar, S.K. Mishra and R. Mohan Naik, *Mater. Today Proc.*, **46**, 2272 (2021); https://doi.org/10.1016/j.matpr.2021.03.735
31. M. Aftab, M.Z. Butt, D. Ali, Z.H. Aftab, M.U. Tanveer and B. Fayyaz, *Environ. Sci. Pollut. Res. Int.*, **29**, 3840 (2022); https://doi.org/10.1007/s11356-021-15945-5
32. Y. Zhang, B. Mahdavi, M. Mohammadhosseini, E. Rezaei-Seresht, S. Paydarfard, M. Qorbani, M. Karimian, N. Abbasi, H. Ghaneialvar and E. Karimi, *Arab. J. Chem.*, **14**, 103105 (2021); https://doi.org/10.1016/j.arabjc.2021.103105
33. B.H. Shnawa, P.J. Jalil, S.M. Hamad and M.H. Ahmed, *Bionanoscience*, **12**, 1264 (2022); https://doi.org/10.1007/s12668-022-01028-3
34. S. Haq, S. Dildar, M.B. Ali, A. Mezni, A. Hedfi, M.I. Shahzad, N. Shahzad and A. Shah, *Mater. Res. Express*, **8**, 055006 (2021); https://doi.org/10.1088/2053-1591/abfc7c